

Silicon Pad Detectors for the PHOBOS Experiment at RHIC

R. Nouicer^a, B. B. Back^b, R. R. Betts^a, K. H. Gulbrandsen^c,
B. Holzman^a, W. Kucewicz^a, W. T. Lin^d, J. Mülmenstädt^c,
G. J. van Nieuwenhuizen^c, H. Pernegger^c, M. Reuter^a,
P. Sarin^c, G.S.F. Stephans^c, V. Tsay^e, C. M. Vale^c,
B. Wadsworth^c, A. H. Wuosmaa^b, B. Wyslouch^c

^a *Department of Physics, M/C 273, University of Illinois at Chicago, 845 West
Taylor St., Chicago, IL 60607-7059, USA*

^b *Physics Division, Argonne National Laboratory, 9700 South Cass Ave., Argonne,
IL 60439-4843, USA*

^c *Massachusetts Institute of Technology, 77 Mass. Ave., Cambridge, MA 02139,
USA*

^d *High Energy Physics Group, National Central University, Department of Physics,
32054 Chung-Li, Taiwan*

^e *Miracle Technology Co. Ltd., Hsin-Chu, Taiwan*

Abstract

The PHOBOS experiment is well positioned to obtain crucial information about relativistic heavy ion collisions at RHIC, combining a multiplicity counter with a multi-particle spectrometer. The multiplicity arrays will measure the charged particle multiplicity over the full solid angle. The spectrometer will be able to identify particles at mid-rapidity. The experiment is constructed almost exclusively of silicon pad detectors. Detectors of nine different types are configured in the multiplicity and vertex detector (22,000 channels) and two multi-particle spectrometers (120,000 channels). The overall layout of the experiment, testing of the silicon sensors and the performance of the detectors during the engineering run at RHIC in 1999 are discussed.

1 Introduction

The Relativistic Heavy Ion Collider (RHIC) at Brookhaven National Laboratory will open a new horizon for Ultra-Relativistic Heavy-Ion physics, to explore highly excited dense nuclear matter under controlled laboratory conditions at a center-of-mass energy of 200 AGeV. At this energy, it is speculated

that a plasma of deconfined quarks and gluons (QGP) will be formed following the initial series of nucleon-nucleon collisions. The QGP subsequently expands, cools and passes into the normal hadronic phase which itself expands until the hadrons cease to interact with each other at the freeze-out stage. A number of signatures of the formation of the deconfined phase have been proposed [1–3]. It is generally thought that a single signature will be insufficient to provide the evidence for the QGP. Rather, the simultaneous observation of several of the proposed signatures, particularly on an event-by-event basis, will be required. PHOBOS seeks to address these questions in a timely fashion by focusing on measurements of hadronic observables for a very large sample of events.

2 PHOBOS detector

The PHOBOS detector consists of a 4π multiplicity array, vertex finding detectors, two multi-particle tracking spectrometers, a set of plastic scintillator time-of-flight (TOF) walls, and trigger detectors. A schematic diagram of the experiment, showing most of these elements is shown in Fig. 1. The experiment is constructed almost exclusively of silicon pad detectors. Which have the advantage as providing simultaneously good position resolution, low multiple scattering in the detector and good energy loss resolution. The multiplicity array consists of an octagonal barrel of silicon pad detectors surrounding the beam pipe, and six rings of silicon pad detectors. This array covers the pseudo-rapidity range of $|\eta| \leq 5.3$. The multiplicity detector will provide event-by-event charged-particle multiplicity distributions which can be used to select interesting events for further study. The multiplicity distributions are interesting in their own right, containing information on multiplicity fluctuations and correlations, which potentially can be related to some of the proposed signatures of the QGP. The vertex detectors consist of two sets of silicon pad sensors situated above and below the beam line in the interaction region. Each set consists of two layers of silicon sensors with 4 sensors in the inner layer and 8 sensors in the outer layer as seen from the interaction region. The silicon vertex finder will be able to determine the position of the interaction point with an accuracy of $50 \mu\text{m}$. The spectrometers consist of planes silicon pad detectors positioned on either side of the beam. Some of these planes lie within a 2T magnetic field. The spectrometers are able to measure and identify particles with transverse momenta as small as to $50 \text{ MeV}/c$ for pions. The spectrometer will determine the particle momentum by measuring the track curvature and the particle type by the dE/dx method. The particle identification capability is further enhanced by two TOF walls behind the spectrometer. Finally, trigger counters consisting of two disks of 16 Čerenkov radiators, and two sets of plastic scintillator counters (paddle counters), are arranged around the beam pipe. The paddle counters are designed to trigger on peripheral collisions and to give a first approximation of the event centrality.

2.0.1 Design of Silicon Pad Detectors

The silicon pad detector is a single sided, AC coupled, detector that uses a double-metal layer to route the signals from the pads to the bonding area at the edge of the sensor. The wafer layout is conceptually similar to one used in CERN experiment WA98[4]. The p+ implants are rectangular pads providing two-dimensional position information. The implants are biased via polysilicon resistors which are connected to a common bias line. A schematic diagram of the cross section of one pad of the silicon detector is presented in Fig. 2. The coupling capacitor between the first metal layer (Al) and the implant layer is formed by a 0.2 μm thick layer of silicon Oxide-Nitride-Oxide (ONO). Each pad from this array is read out by a second metal line that connects to the Metal 1 pad through a via and runs to the bonding pad. The active area of the silicon wafer is surrounded by a guard ring. The double metal layer has the advantage that the readout structure is integrated on the sensor without additional material. The full detector surface can be used for routing the signal lines to the sensor edge to a single row or multiple rows of bonding pads, permitting the use of standard readout chips. Nine different sensor types are used. The geometric characteristics of the different types of the sensors are presented in Table 1. A schematic layout of some of the silicon sensors used are shown in Fig. 3 and more details about silicon sensors are presented in reference [5,6].

Table 1
Physical specifications of the PHOBOS silicon pad sensors

Detector System	Sensor Type	Active Area [mm ²]	Number of Pads	Pad Size [mm ²]
Spectrometer	1	70.0 x 22.0	70 x 22	1.0 x 1.0
	2	42.7 x 30.0	100 x 5	0.4 x 6.0
	3	42.7 x 60.0	64 x 8	0.7 x 7.5
	4	42.7 x 60.0	64 x 4	0.7 x 15.0
	5	42.7 x 76.0	64 x 4	0.7 x 19.0
Multiplicity	Octagon	34.9 x 81.3	30 x 4	2.75 x 8.75
	Ring	3600	8 x 8	20 - 105
Vertex	Inner	60.6 x 48.18	4 x 256	0.5 x 12.1
	Outer	60.6 x 48.18	2 x 256	0.5 x 24.1

2.0.2 Testing and Acceptance Criteria of the Silicon Sensors

The silicon sensors were produced by the Miracle Technology Co, Taiwan under supervision of the National Central University (NCU), Taiwan. The dicing

and initial inspection was carried out at NCU. Subsequent testing of the characteristics of the Silicon wafers was conducted at the University of Illinois at Chicago (vertex, octagon and ring wafers) and at Massachusetts Institute of Technology (spectrometer wafers).

This testing procedure was performed using a computer controlled probe station running LabView (National Instruments), which can write the results directly into a central Oracle database [7]. The probe station is equipped with Keithley units for current and voltage measurements as well as with capacitance-meters for capacitance measurements of the sensor. The following tests are performed on each sensor :

- *IV Test* : The leakage current is measured as a function bias voltage applied to the active area and the guard ring separately. The backplane voltage is applied through the vacuum jig. Sensors with less than $5 \mu\text{A}$ current for the full active area at full depletion voltage, typically around 70 V and with stable guard ring current are accepted.

- *PN Test* : The sensor depletion voltage is measured on a p-n diode test structure adjacent to the sensor on the same production wafer. This measured value for the depletion voltage was cross-checked with the results of tests with radioactive source carried out on the actual sensor. For most sensors, the depletion voltage was approximately 70 Volts.

- *Polysilicon Test* : The polysilicon bias resistor was measured for each wafer on two identical test structures on the wafer. These test structures consist of a chain of resistors identical to those used to bias each pad. We measure the current-voltage characteristic for both test structures and accept sensors with pad bias resistance larger than $1 \text{ M}\Omega$.

- *Pinhole Test* : Pinholes, or connections between the two metal layers through the first dielectric layer, are detected by measuring the current between the bonding pad and the bias line. The bias line is kept at ground potential and the bond pads are held at - 5V. For functional oxides, the measured current is zero. This measurement was done for each pad.

- *CV Test* : The functionality of the readout line is checked by measuring the capacitance between each pad and the detector backplane, while the sensor is fully depleted. For functional lines a characteristic capacitance pattern is observed, which largely depends on the readout line geometry and routing. Broken or shorted lines clearly exhibit a different capacitance which can easily be distinguished from that of functional lines. We allow a total of 3 % defective channels (sum of thin oxide defects and readout line defects) for each sensor.

2.0.3 Readout Electronics

The readout of all PHOBOS silicon detectors is based on the VA-HDR-1 chip, a "Viking" type chip manufactured by IDEAS [8]. We use it in a 64-channel and a 128-channel version depending on the sensor granularity. The VA-HDR-1 chip was chosen as it is commercially available and provides a large dynamic range, with input signals up to 400 fC, i.e. more than 100 times the energy

loss of minimum ionizing particle (MIPs). The VA-HDR-1 chips are mounted on a hybrid. These hybrids are ceramic in the case of the vertex and spectrometer detectors, and multilayer printed circuit boards for the multiplicity detectors. Each hybrid carries one or more chips with the chip inputs directly wire bonded to the sensors. The hybrid also has a small number of passive components to adjust the chip supply currents from common voltage rails and to filter the power supplies. The data are read out by Front End Controllers (FEC's) which digitize the differential analog signals in a 12 bit ADC running at up to 5 MHz and store the ADC output in a FIFO. The digitized data are passed through a G-Link connection and multiplexing boards to a Mercury Raceway system [9] in which multiple PowerPC processors work concurrently on the data reduction. The FEC's also monitor chip supply voltages, detector bias voltage and leakage currents. The monitoring values are automatically transmitted together with the ADC data. Finally, the processed data are sent to a workstation where they can be analyzed.

2.0.4 Module Assembly and Tests

After each chip is tested and accepted, it is manually attached with conductive glue to the hybrid. The chip control side is wire bonded to the hybrid. After bonding, the hybrid is tested by reading the pedestal, measuring the chip noise and running a full calibration cycle for each channel. Following these tests, the sensor is glued to the hybrid. Finally, the sensor is wire bonded to the chip input. After assembly, the functionality of the completed module is tested in the same manner as the unassembled hybrid. In addition, each module is tested with an electron source ^{113}Sn ($E_{e^-} = 363 \text{ keV}$ and 380 keV), which gives information about the full depletion voltage. The signal distribution from one pad of a ring-counter sensor from a ^{113}Sn source is presented in Fig. 5. The response of a vertex sensor to minimum ionizing particles is shown in Fig. 6, which displays an energy-loss spectra for cosmic-ray muons. The peak of the minimum ionizing energy distribution occurs at approximately 80-90 keV. The width of the curve represented in the Fig. 6 is due to Landau Fluctuations. The signal signal-to-noise ration is approximatively 15. These silicon detectors have been also used during the engineering run in 1999. The stability of one octagon module during this period is illustrated in Fig. 7.

2.1 Performance of Silicon pad Detectors during Engineering Run at RHIC

During the engineering run of June 1999 at RHIC, 13 octagon modules, one half of the top layer of the inner vertex array (one module), one quarter of the top layer of the outer vertex array (two modules) and four first planes of spectrometer were installed. During this period, Au beam at injection energy (10.8 GeV/n) was circulated in each of the RHIC rings but not simultaneously. During this exposure, the silicon pad detectors showed low noise and very good stability in pedestal and gain. The average pedestal and noise per channel for one octagon module during running are presented in Fig. 7.

3 Summary

Since the signature of the quark-gluon plasma cannot be predicted unambiguously, PHOBOS is initially attempting to study these collisions in an unbiased way. Therefore PHOBOS will study the production of all types of hadronic particles. The majority of the emitted charged hadrons will be detected by the multiplicity detector, which covers almost 4π of solid angle. This permits us to study their distribution in the pseudo-rapidity range of $|\eta| \leq 5.3$ on an event-by-event basis. One percent of all emitted particles will be studied in detail by the two-arm magnetic spectrometer in the mid-rapidity region, where the highest energy densities are expected. In the spectrometer, particles will be momentum analysed and identified by energy loss measurements in the Silicon layers. The identification of higher momentum particles will be augmented by time-of-flight measurement.

For the silicon pad detectors, the sensor quality was demonstrated to be adequate for the required physics measurement. The sensor production, testing and assembly have been completed on schedule. Source and beam tests show an acceptable signal-to-noise ratio around 15. The expected capacitive coupling between the channels gives a modest crosstalk of less than 1%.

Currently, the silicon pad detectors of PHOBOS are ready for implementation in the RHIC research program. The full multiplicity detector, the vertex detectors and one arm of the spectrometer are ready and will be installed when RHIC physics running starts in June 2000.

References

- [1] C.P.Singh Phys. Rep. 236(1993)147.
- [2] J. Harris and B. Muller. Ann. Rev. Nucl. Part. Sci. 46(1996)71.
- [3] J. Alam, S. Raha and B. Sinha. Phys. Rep. 273(1996)243.
- [4] W.T. Lin et al., Nucl. Inst. and Meth. A 389 (1997)415.
- [5] B. Back et al., Nucl. phys B78(1999)245.
- [6] Heinz Pernegger, Nucl. Instr. and Meth. A 419 (1998)549.
- [7] ORACLE, 500 Oracle Parkway, Redwood Shores, CA 94065, U.S.A.
- [8] Integrated Detector and Electronics, Veritasvein 9, N-1322 Hovik, Norway.
- [9] Mercury Computer Systems, Inc., 199 Riverneck Road, Chelmsford, MA 01824-2820, USA.

Fig. 1. Schematic drawing of the PHOBOS detector showing the major components. For reasons of clarity, the top half of the magnet has been removed.

Fig. 2. Schematic diagram of the cross section on one pad of the PHOBOS silicon detectors.

Fig. 3. Schematic layout of some of the silicon sensors used in PHOBOS.

Fig. 4. Test results of one octagon silicon sensor. The (a), (b) and (c) plots represent IV test, polysilicon test and CV test, respectively.

Fig. 5. Signal distribution on one pad of the ring counter using a ^{113}Sn source.

Fig. 6. Energy loss distribution for cosmic-ray muons on one vertex sensor.

Fig. 7. Average pedestal per channel (a) and average noise per channel without common mode noise subtraction (b) for one octagon module installed during the engineering run at RHIC.

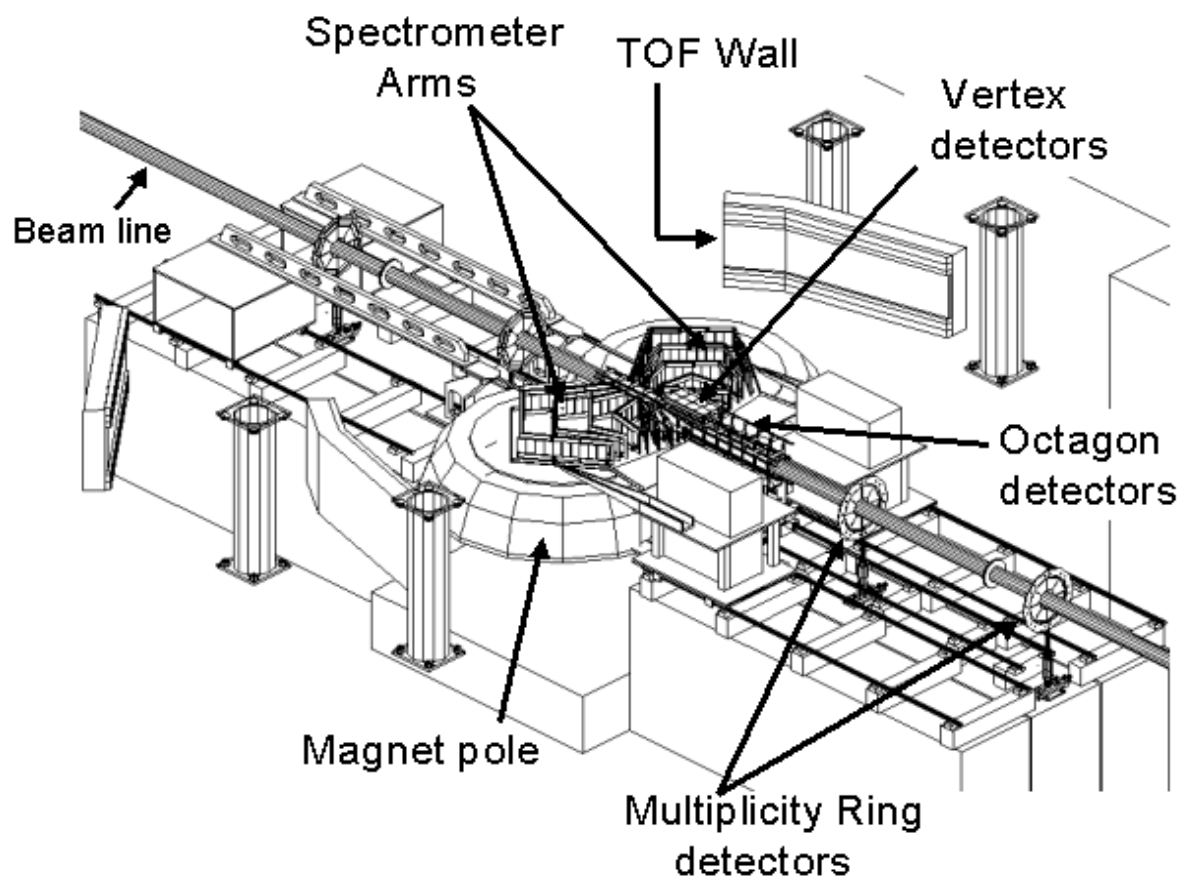


Fig.1

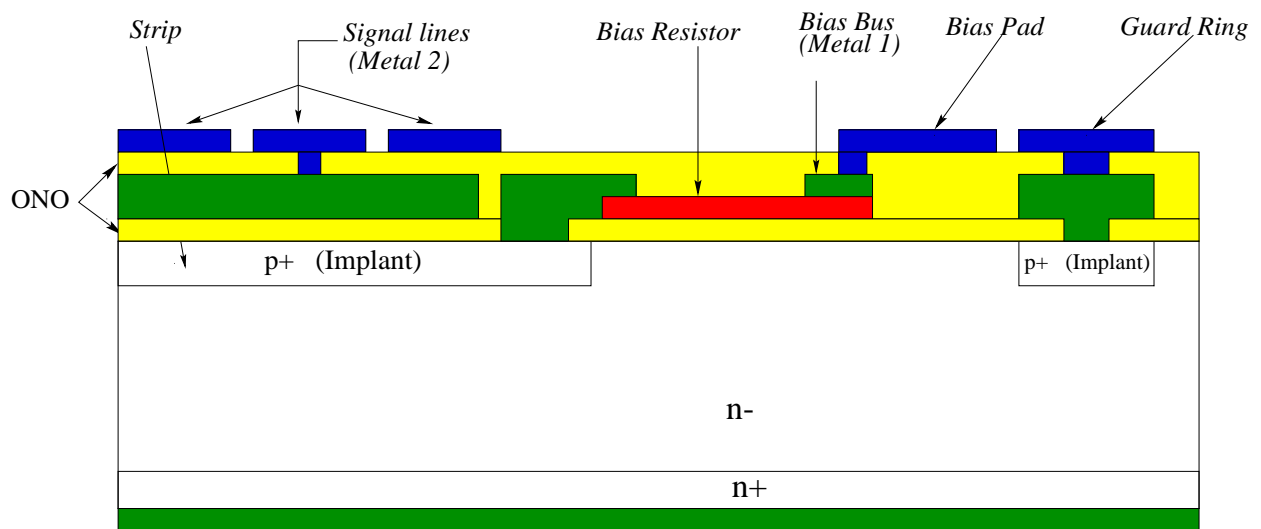


Fig.2

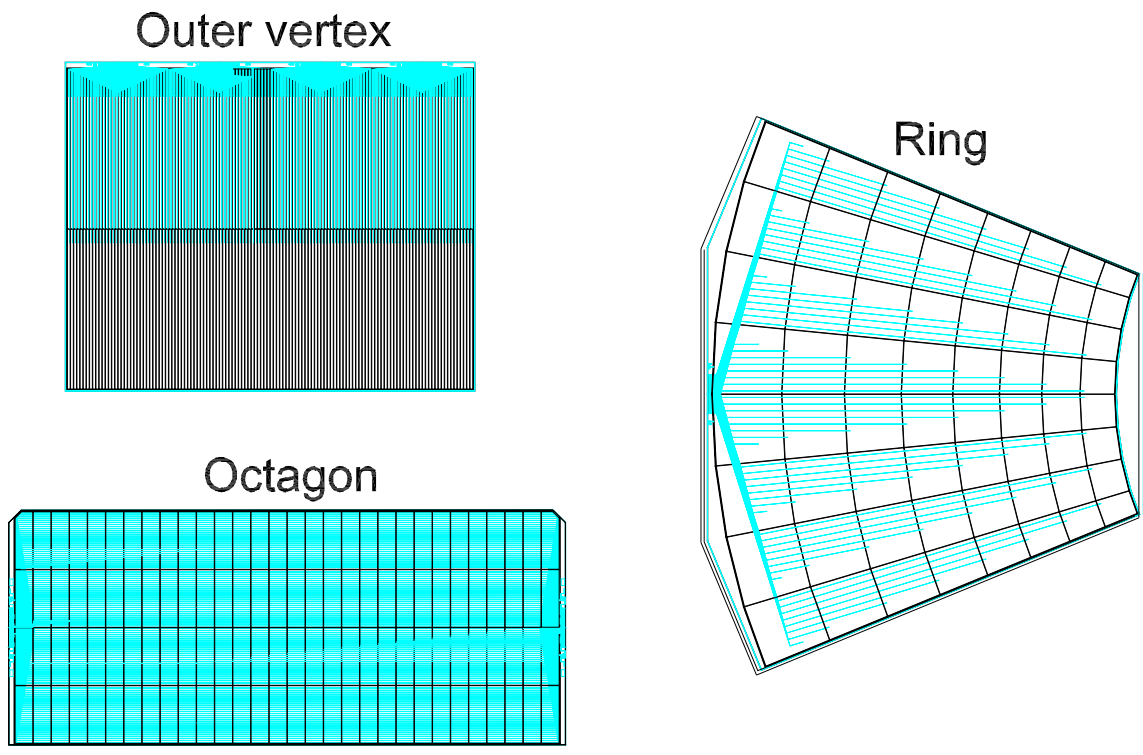


Fig.3

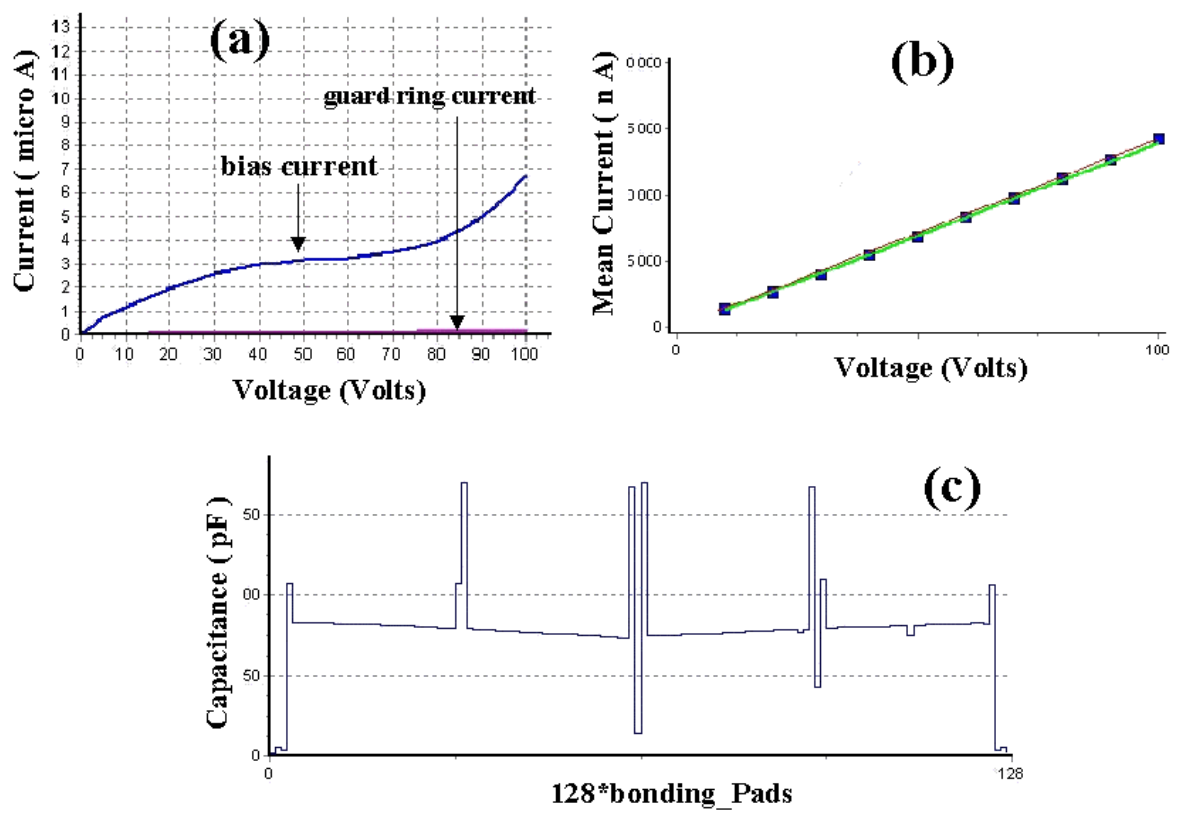


Fig.4

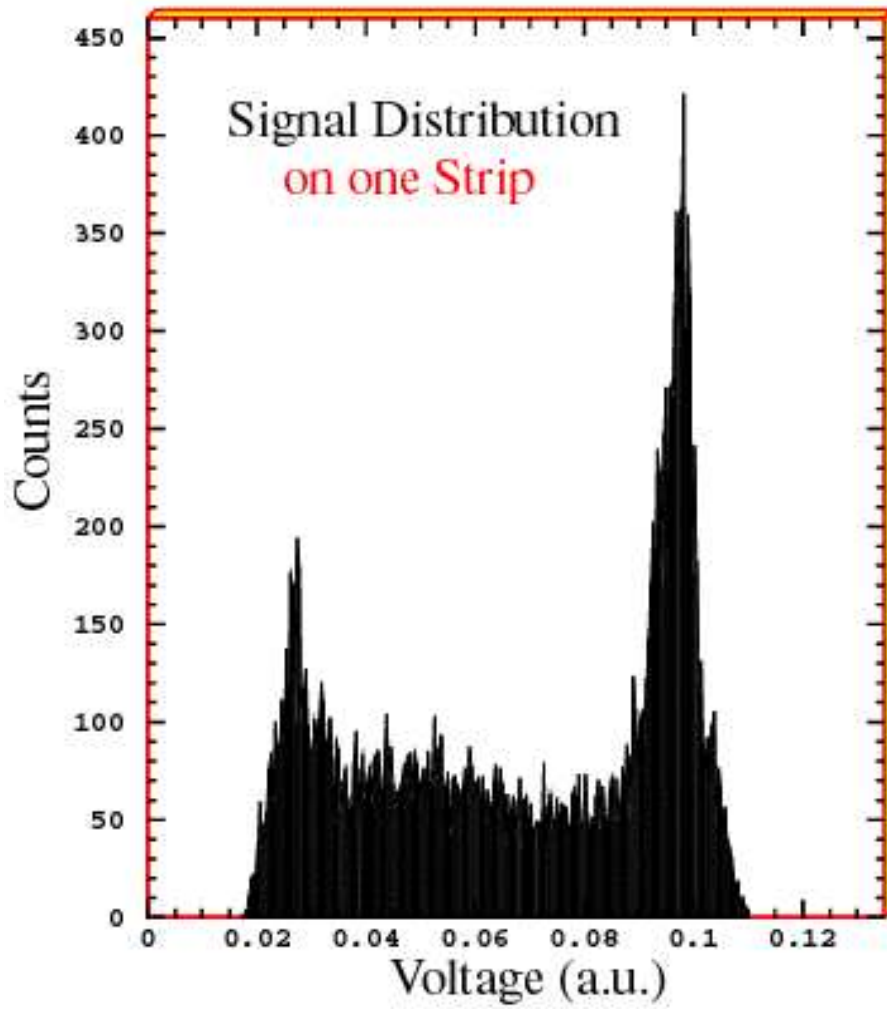


Fig.5

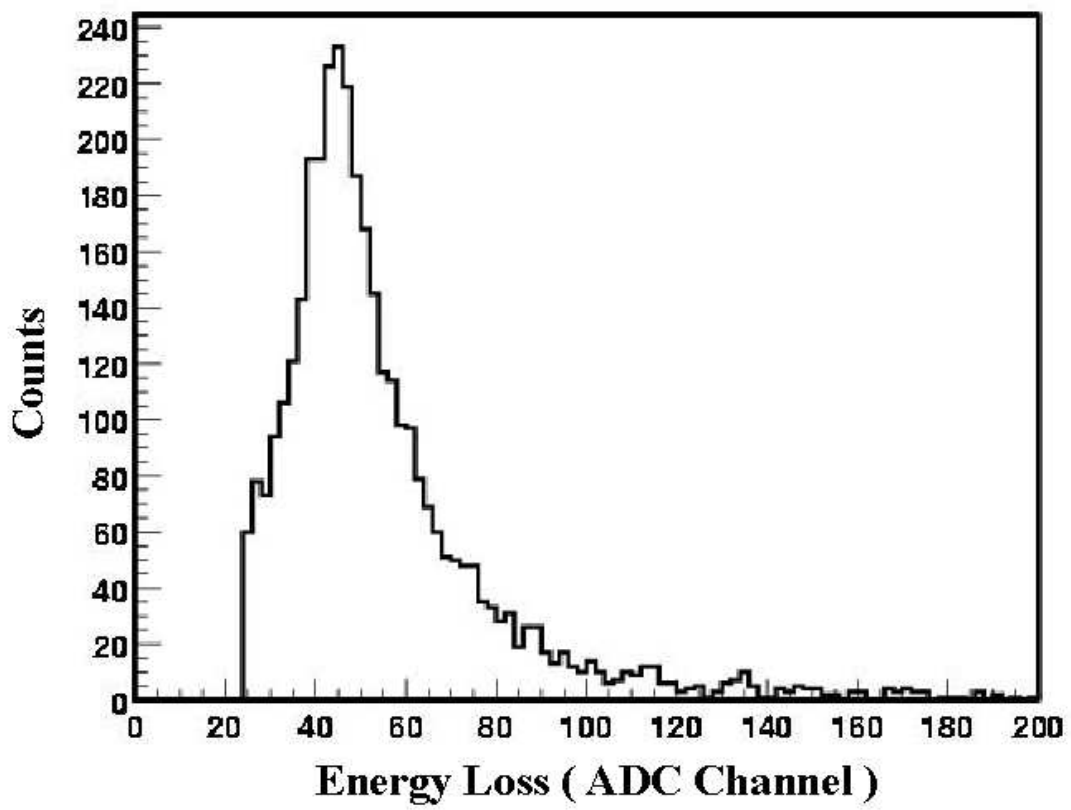


Fig.6

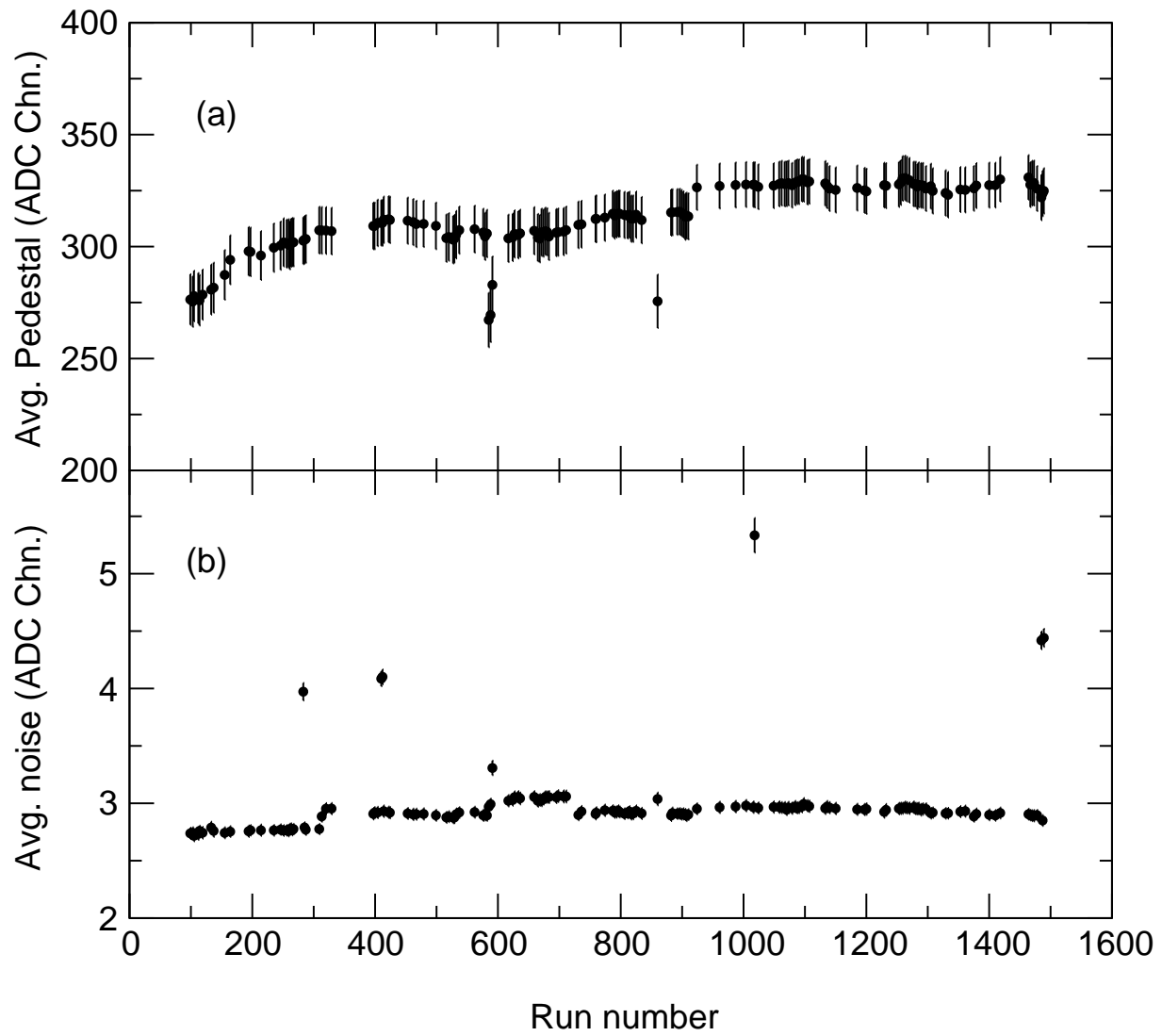


Fig.7